archives
of thermodynamics
Vol. **34**(2013), No. 1, 41–53
DOI: 10.2478/aoter-2013-0003

Numerical modeling of CO_2 separation process

LESZEK REMIORZ*
SEBASTIAN RULIK
SŁAWOMIR DYKAS

Silesian University of Technology Institute of Power Engineering and Turbomachinery Konarskiego 18, 44-100 Gliwice, Poland

Abstract Paper presents the results of numerical modelling of a rectangular tube filled with a mixture of air and CO_2 by means of the induced standing wave. Assumed frequency inducing the acoustic waves corresponds to the frequency of the thermoacoustic engine. In order to reduce the computational time the engine has been replaced by the mechanical system consisting of a piston. This paper includes the results of model studies of an acoustic tube filled with a mixture of air and CO_2 in which a standing wave was induced.

Keywords: CO_2 separation; Thermoacoustic; CFD

1 Introduction

Carbon dioxide (CO_2) belongs, together with water vapour, methane, chlorofluorocarbons, ozone and nitrogen oxides, to a group called greenhouse gases. These gases are responsible for the accumulation of heat in the atmosphere of the Earth. It is estimated that CO_2 has a significant, about 50% share in this effect [4]. This results from its strong absorption of infrared radiation, as well as from the large quantities of CO_2 present in the atmosphere due to its emissions in conventional processes of heat and electricity generation. Therefore, the efforts of research circles are strongly focused on the methods to reduce CO_2 emissions into the atmosphere by

*Corresponding Author. E-mail: leszek.remiorz@polsl.pl

means of the improvement in the efficiency of power engineering systems and of the introduction of CO_2 capture technologies.

Separation methods of CO_2 are divided into precombustion and post-combustion techniques, fuel oxygen combustion, and the use of fuel cells to reduce CO_2 emissions [4,5]. The CO_2 separation process itself can be divided into absorption, adsorption, membrane separation, and cryogenic methods. Each of these processes can be used in all separation methods. Apart from the above-mentioned methods, which are already at a certain level of research advancement, other separation methods based on different physical phenomena are being developed. One of them is separation which makes use of the acoustic or thermoacoustic wave. The thermoacoustic phenomenon was described for the first time by Lord Rayleigh in 1878 [9]. The original description comes down to the statement that, if heat is added to gas when it is compressed the most, or extracted when the gas is expanded, an oscillatory wave will be formed. Naturally, the description does not specify the mechanism of the thermoacoustic wave formation; it merely presents a description of the concept of induction of such a wave. A scientific investigation of this phenomenon can be found in studies conducted in the 80s and 90s of the 20th century. In particular, they are the works of Rott from the 60s and 70s, and Weatley and Swift from the 80s and 90s, and others [1–3,6]. The simplest method to induce a thermoacoustic wave is the application of the Rijke tube [8,9]. From the thermodynamic point of view, the thermoacoustic phenomenon realises the Stirling cycle and, as such, it can be considered as a right- or left-running cycle, i.e., as the engine cycle or the cycle of the cooler. Both cases have already found application in prototype devices such as thermoacoustic engines and coolers, natural gas liquefaction facilities and many others. Studies of the thermoacoustic wave have also shown that, in certain conditions, the wave can be used in the gas separation process. The aim of this study is to investigate the possibility of using the thermoacoustic wave in CO_2 separation processes. It should be treated as preliminary research for further, more detailed, analyses. In particular, the aim of this study is to start a numerical model of the separation process, and its parametric analyses.

2 Thermal diffusion

Thermal diffusion (thermodiffusion, the Soret effect) is a process of disturbance in the mixture homogeneity which is caused by the difference in temperatures in the medium, and which consists in the movement of particles in the mixture or solution resulting from the temperature gradient. The Soret effect is explained in Fig. 1. In subsequent time the moving acoustic wave produces a temperature gradient, which in turn causes a momentary disturbance in the contents of individual components in the mixture. If the temperature gradient direction is properly correlated with the direction in which the mixture particles move, a lasting effect of separation can be obtained.

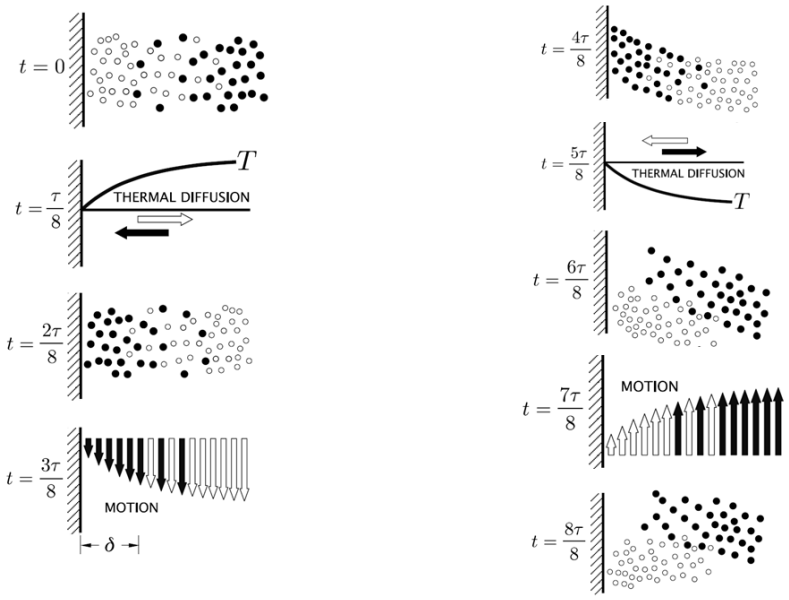

Figure 1. Thermal diffusion mechanism produced by the temperature gradient between the wave front and the tube wall [10]: t – time, T – temperature, τ – period of oscillation, δ – thickness of the boundary layer.

As it can be seen in Fig. 1, in subsequent time the moving front of the pressure wave produces a temperature gradient towards the tube walls, which entails a momentary separation of the mixture. It should be noted that, apart from this effect, there is also a purely mechanical impact of the wave on the mixture particles.

3 CFD model, parametric analysis

The numerical model of CO_2 separation was developed with the use of a computational fluid dynamics commercial code Ansys-CFX13 [11]. The scheme of the computational domain is presented in Fig. 2. The following dimensions of the computational region are adopted: $x = 20$ mm, $y = 50$ mm, $z = 1000$ mm. Both for the lateral and the top, as well as, bottom areas, boundary conditions were assumed as symmetry. Therefore, the model does not take account of the impact of the walls and the friction related to it on the behaviour of the acoustic wave.

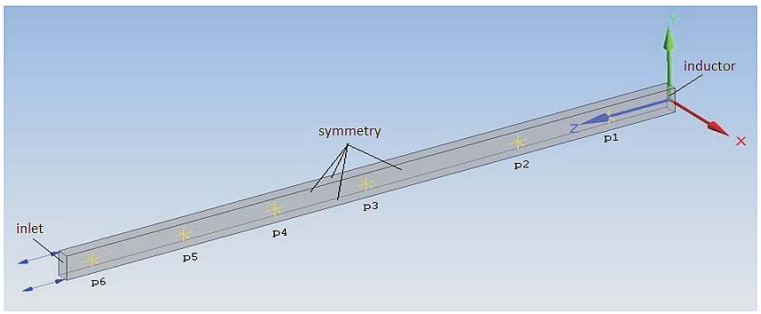

Figure 2. View of the rectangular tube, with dimensions $20 \times 50 \times 1000$ mm, adopted for the calculations.

Calculations for a thermoacoustic tube with similar dimensions have confirmed that there was no significant impact of this assumption on the calculation results [7]. However, the assumed symmetry (Fig. 2) has a substantial impact on the computation time, which becomes definitely shorter. As an enforcement, a sinusoidally changeable location of the closed end of the tube was assumed, while the other tube end remained open. The adopted computational model thus realises a computational scheme whose mechanical analogy is shown in Fig. 3. It is a long cylinder closed at one end with a movable piston. The piston location is described by the following equation:

$$x_t = s\cos(2\pi f t_s) \ , \tag{1}$$

where x_t is the change in the location of the mesh enforcing (piston) oscillations, s, and f is the maximum shift and oscillation frequency, respectively, and t_s is the simulation time. However, this equation does not take account of the fluctuations of the connecting rod, and the changes in the piston location resulting from them. The change in location is caused only by

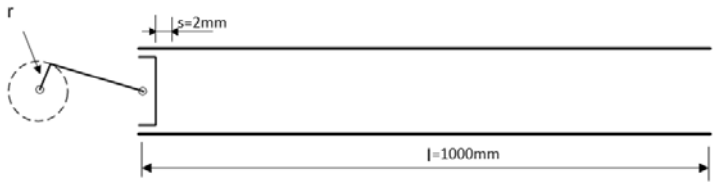

Figure 3. Mechanical analogy of the computational model.

the rotation of crank r. The maximum shift from the initial state was assumed at $s = 2$ mm. The tube was filled with a mixture of air and CO_2 with volume contents of 85 and 15%, respectively. At the outlet section, an open boundary condition was assumed with inlet pressure equal to 0 Pa (compared to reference pressure). The open boundary condition allows a two-way flow of gas, depending on the pressure distribution.

For the case under analysis, the mechanical enforcement of the acoustic wave was performed by the method of so-called movable meshes implemented within the code ANSYS-CFX. In our case, this allows a simplified modelling of the sound source. The target source being a thermoacoustic engine. It was assumed that one of the walls of the calculation area (the inductor) oscillated with a strictly defined frequency. This results in a local deformation of the numerical mesh. The oscillations are responsible for the formation of an acoustic wave in the device. At the same time, on the inductor wall itself, the velocity value is assumed as zero (the velocity node), and the pressure at this point reaches its maximum value (the pressure antinode). The basic data of the numerical simulation are: frequency $f = 85.25$ Hz, temperature $T = 300$ K, reference pressure $p = 0.1$ MPa. Assumed physical model consists of two continuous phases, air and CO_2, governed by Euler-Euler approach with the volume fraction 85 and 15%, respectively. The adopted basic time step of 3.91×10^{-4} s corresponds to 30 iterations per single acoustic wave period. The impact of time discretisation will also be discussed in detail in one of the sections below. Additionally, in the case under consideration, the inductor oscillation frequency was adopted at 85.25 Hz – the value resulting from the frequency of the standing wave for this tube. The aim of the numerical analysis was to determine whether CO_2, would be concentrated due to the effect of the acoustic wave, and whether the mixture homogeneity would be disturbed. For this purpose, the CO_2 content at individual locations was analysed. Figure 4 presents the obtained results, which show that CO_2 concentration at

certain locations increases with time, while at other locations it decreases. After 2.5 s the carbon dioxide content increases near the inductor itself and reaches the value of approx. 0.28, whereas near the outlet area the CO_2 content is approx. 0.08. At the same time, all thermodynamic values and CO_2 content at individual locations oscillate around their local average values. However, the oscillations are small compared to the obtained differences in CO_2 contents. The control points were placed at a distance of 0.1, 0.25, 0.5, 0.65, 0.8, and 0.95 m from the inductor.

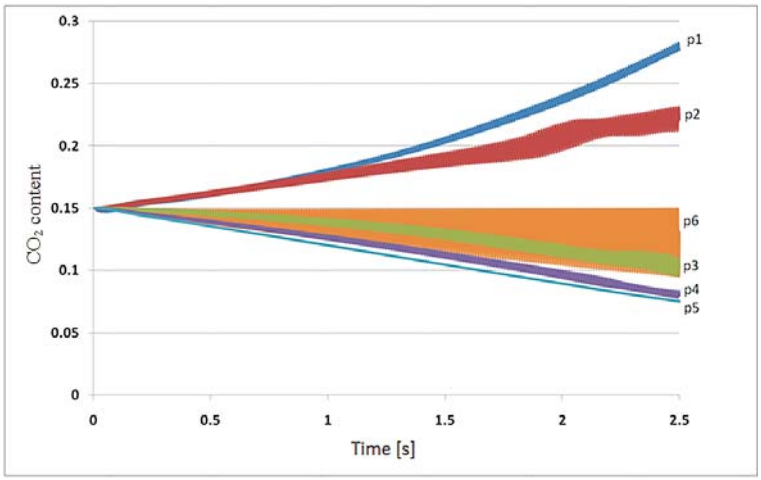

Figure 4. The CO_2 contents at control points p1–p6 for mesh I.

4 The impact of space discretisation in six control points

In order to analyse the impact of space discretisation, three different sizes of orthogonal numerical meshes were assumed: I – 2.500, II – 10.000, and III – 40.000 finite volumes. In the analysed cases, the size of meshes was enlarged proportionally in all three directions. Figures 4 and 5 present the content of CO_2 at six individual control points for the three numerical meshes under consideration. It can be noticed that for the smallest mesh (mesh I) the course of CO_2 contents as a function of time is uniform. The differences in CO_2 contents between the far ends of the device gradually increase. The maximum CO_2 concentration is approx. 0.28, and the minimum is approx. 0.08. For the second numerical mesh the values are 0.3

and 0.08, respectively. At the same time, the course of CO_2 contents for point p2 is characterised by a slight change in amplitude in the final part of the considered time interval.

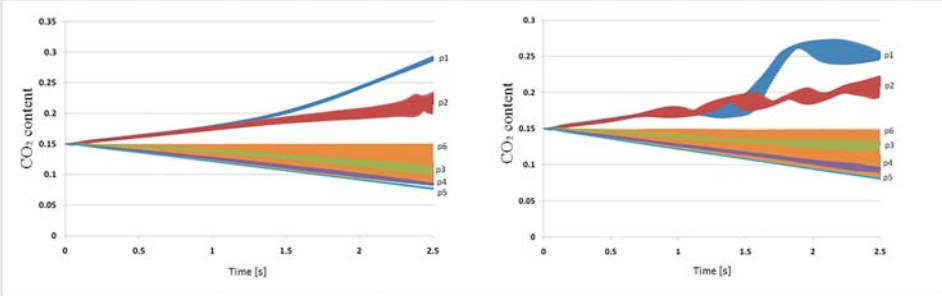

Figure 5. The CO_2 content for mesh II (left) and mesh III (right) at control points p1–p6.

The last numerical mesh which was analysed (Fig. 5) was composed of 40.000 elements. In this case, it can be seen that CO_2 content at individual locations are characterised by abrupt changes in values and in the amplitude. It is best visible for control points p2 and p3, which are situated close to the outlet section. It can also be seen that the CO_2 content value for the point p1 is stabilised at a steady level. In this case, the maximum CO_2 concentration is approx. 0.25, and the minimum is approx. 0.08. Figure 6 presents CO_2 content obtained for the three used numerical meshes. The contents were calculated for four simulation times: 0.5, 1, 2, and 2.5 s. On the basis of the presented characteristics, it can be stated that the impact of the numerical mesh at the initial stage of the simulation is slight. For all separated time instants, a sufficient consistency of results is obtained. However, the differences grow as the numerical simulation proceeds. For time 2.5 s, discrepancies appear for all control points. They are the biggest for points p1 and p3. For point p3 the difference between the results obtained for different numerical meshes reaches the value of approx. 15%.

5 The influence of time discretisation

In addition to the determination of the space discretisation effect, the impact of the adopted time step on the distribution of the CO_2 content along the device was checked. For this purpose, similarly as before, four characteristic time points were selected, and the calculations were conducted with

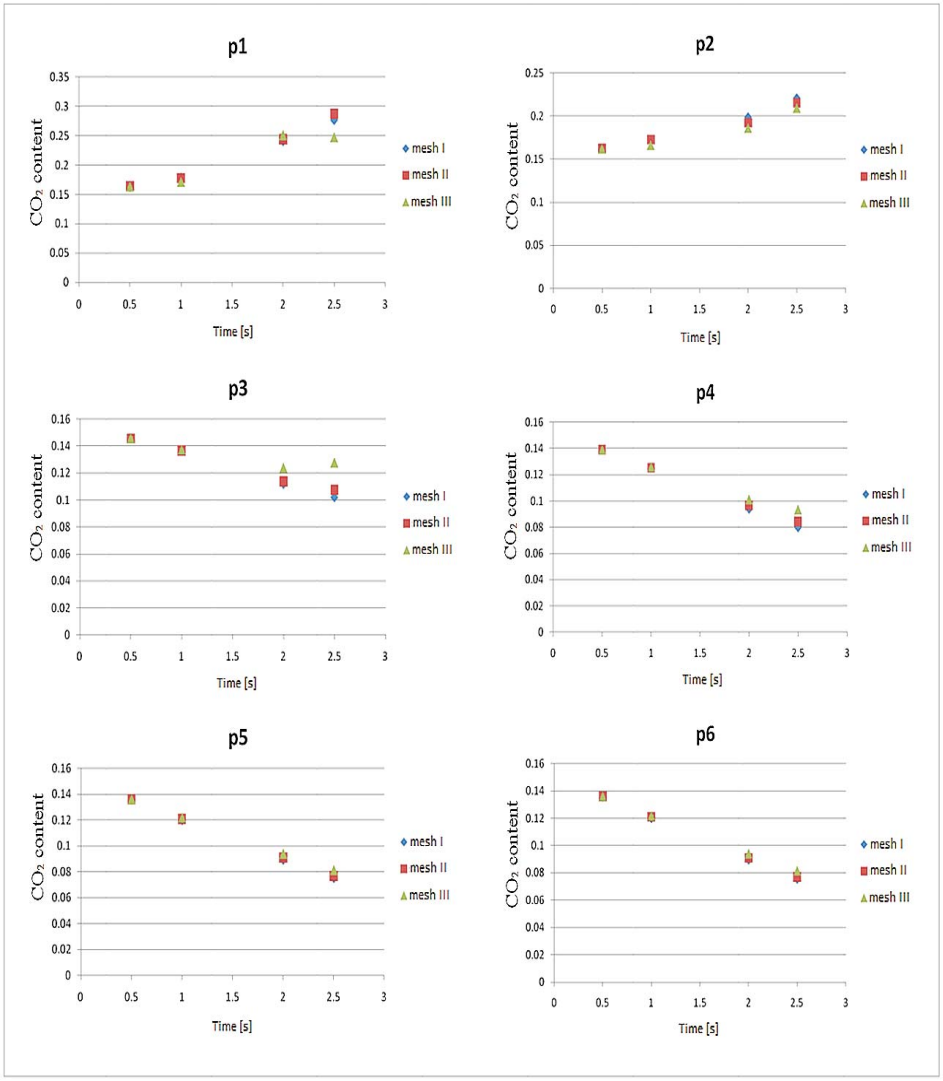

Figure 6. The CO_2 content at control points p1–p6 at four times (0.5, 1, 2, and 2.5 s) obtained with three different meshes.

the use of four different time steps for numerical simulation. The time steps in this case were determined on the basis of the following dependence:

$$t = \frac{1}{fn}\,, \tag{2}$$

where t is the time step, f is the inductor oscillation frequency, n is the assumed number of iterations per acoustic wave period; n was assumed at 15, 30, 60, 120, which gives the following time steps: $t_1 = 7.82 \times 10^{-4}$ s, $t_2 = 3.91 \times 10^{-4}$ s, $t_3 = 1.96 \times 10^{-4}$ s, and $t_4 = 9.78 \times 10^{-5}$ s. Figure 7

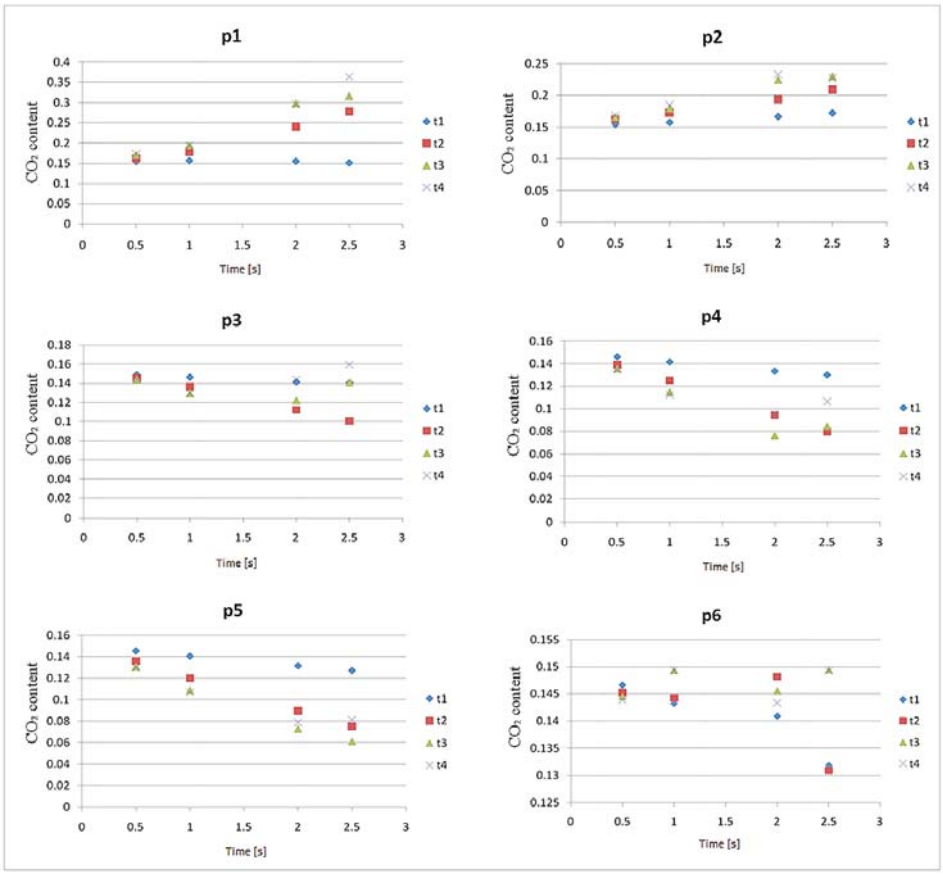

Figure 7. CO_2 content at six control points (p1–p6) at four times (0.5, 1, 2, and 2.5 s), for four different time steps.

presents the obtained calculation results. It can be noticed that the impact of the adopted time step on the CO_2 contents at individual control points is much stronger than in the case of space discretisation. Therefore, the inappropriate selection of the time step, restricted by the time of the calculations themselves, may result in big differences in the obtained results. Significant differences in CO_2 contents depending on the applied time step

occur for all control points under consideration (Figs. 7 and 8). The biggest differences appear for point p1. The discrepancies between the obtained results of the CO_2 content vary from 0.15 to 0.35 for the simulation time of 2.5 s. Smaller differences also appear for the remaining control points. For point p5 the differences are included in the range of 0.06–0.013.

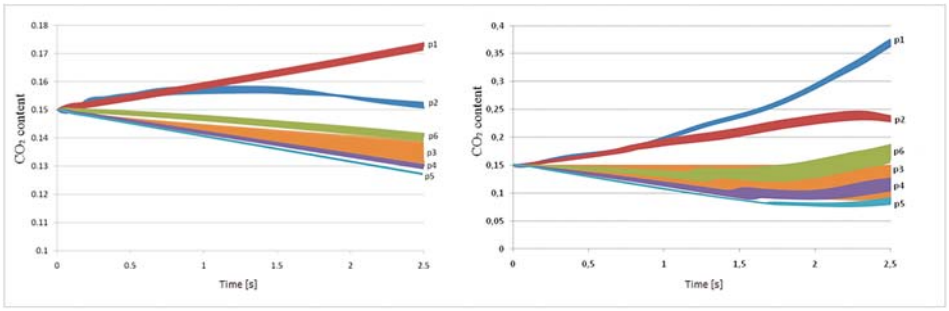

Figure 8. The CO_2 content for time steps 7.81×10^{-4} and 9.78×10^{-5} at control points p1–p6.

6 The impact of average pressure

The impact of average pressure on the CO_2 content at individual control points was analysed within the time range of 0–1.3 s. The following average pressure values in the device were considered: $p_{o1} = 0.1$ MPa, $p_{o4} = 0.4$ MPa, $p_{o2} = 0.2$ MPa, $p_{o5} = 0.5$ MPa, $p_{o3} = 0.3$ MPa, $p_{o6} = 0.6$ MPa. Figure 9 presents the distribution of CO_2 content at control points in the case of application of different values of average pressure. For the initial stage of the simulation it can be observed that the impact of average pressure is slight, but gradually increases with time. The biggest impact of average pressure can be observed for point 5. For simulation time of 1.3 s, the volume content of CO_2 is 14% for pressure p_{03}, and for pressure p_{06} is 10%. However, the conducted analysis shows that the impact of average working pressure on the CO_2 content at individual control points is not unequivocal.

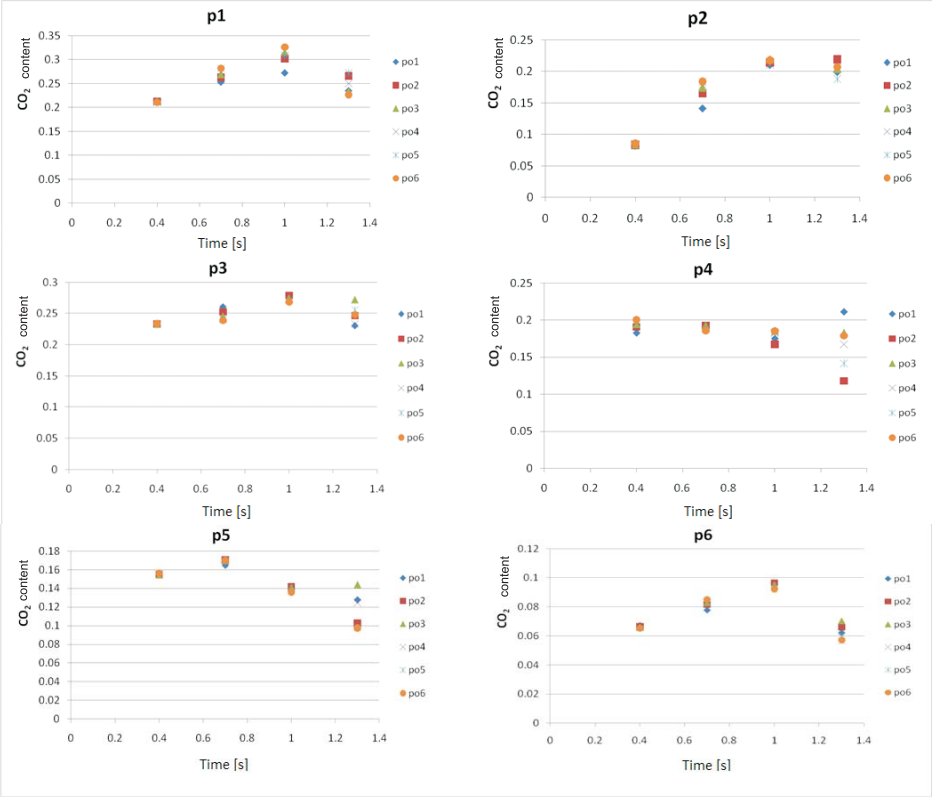

Figure 9. The CO_2 content at six control points for four times (0.4, 0.7, 1, and 1.3 s), depending on reference pressure p_{o1}–p_{o6}.

7 Visualisation of calculation results

The conducted numerical analysis shows that if in the rectangular tube filled with a mixture of air and CO_2 an acoustic wave with an appropriately selected frequency is generated, due to the effect of the wave a slow-changing process of the separation of the gases occurs. The process has a lasting nature with respect to the running acoustic wave, i.e., subsequent wave cycles do not disturb the process, but they rather intensify it. This is shown in Fig. 10. The whole tube is filled with a homogenous mixture of air and CO_2 at instant $t = 0$ s, but after time $t = 0.6$ s, appear the places with an increased concentration of CO_2, and after time $t = 1.2$ s the lasting

inhomogeneity is already clearly visible. Although in the numerical model intense separation process occurred, the obtained result has to be verified by laboratory tests.

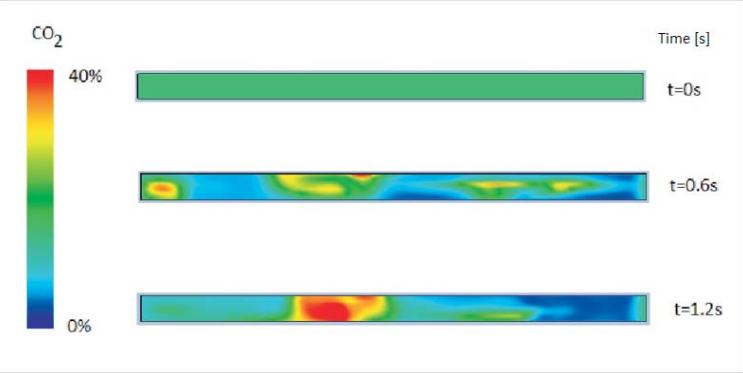

Figure 10. CO_2 separation. Image of the modelled tube at subsequent times: 0, 0.6, and 1.2 s.

8 Conclusions

The results of numerical modelling of an acoustic tube filled with a mixture of air and CO_2 were presented. A rectangular testing tube with dimensions: $20 \times 50 \times 1000$ mm was assumed. One end of the tube was left open, whereas an acoustic wave inductor was modelled at the other end. Due to the effect of an acoustic wave, a disturbance in the mixture homogeneity occurred in the modelled tube. The homogeneity disturbance had a lasting character with respect to the subsequent oscillation cycles in the tube. The observed phenomenon was not qualitatively affected by parameters such as the numerical mesh size, the adopted time step or the pressure in the tube. The separation could be observed regardless of the values of adopted parameters, within the set limits, of course. At the same time, the values adopted for the modelling had an impact on the level and time of separation, which was the case for space and time discretisation in particular. The presented results need experimental verification.

Acknowledgements The results presented in this paper were obtained from research work cofinanced by the National Centre for Research and

Development in the framework of Contract SP/E/1/67484/10 – Strategic Research Programme – Advanced technologies for energy generation: Development of a technology for highly efficient zero-emission coal-fired power units integrated with CO_2 capture.

Received 1 December 2011

References

[1] Geller D.A., Swift G.W.: *Thermodynamic efficiency of thermoacoustic mixture separation*. J. Acoust. Soc. Am. **112**(2002), 2, 504–510.

[2] Swift G.W., Spoor P.S.: *Thermal diffusion and mixture separation in the acoustic boundary layer*. J. Acoust. Soc. Am. **106**(1999), 1794–1800.

[3] Swift G.W. and Geller D.A.: *Continuous thermoacoustic mixture separation*. J. Acoust. Soc. Am. **120**(2006), 5, 2648–2657.

[4] Kotowicz J., Janusz K.: *Ways of CO_2 emissions reduction from energy consuming processes*. Rynek Energii, **1**(2007), 10–18.

[5] Chmielniak T.J., Chmielniak T.: *CO_2 separation from energy processes of fuel conversion*. Sciążko M., Zieliński H. (Eds.): *Thermochemical processing of coal and biomass*. IChPW and IGSMiE PAN Publishers, Zabrze – Kraków 2003 (in Polish).

[6] *United States Patent: Patent No.: US 6,733,569 B2*, May 11, 2004

[7] Remiorz L., Dykas S., Rulik S.: *Numerical modelling of thermoacoustic phenomenon as contribution to thermoacoustic engine model*. TASK **14**(2010), 3, 261–273.

[8] Carrier F.: *The mechanics of the Rijke tube*. Quart. Appl. Math., **12**(1955), 4, 383–395.

[9] Lord Rayleigh: *The Theory of Sound*, II. Dover, New York, 1945.

[10] Spoor P.S. Swift G.W.: *Thermoacoustic separation of a He-Ar mixture*. Phys. Rev. Lett. **85**(2000), 1646–1649.

[11] http://www.ansys.com/